The solution structure of the complex of Lactobacillus casei dihydrofolate reductase with methotrexate

ARTICLE *in* JOURNAL OF MOLECULAR BIOLOGY · MARCH 1998

Impact Factor: 4.33 · DOI: 10.1006/jmbi.1997.1560

9 AUTHORS, INCLUDING:

Vladimir Polshakov
Lomonosov Moscow State University
70 PUBLICATIONS **521** CITATIONS
SEE PROFILE

Igor L Barsukov
University of Liverpool
79 PUBLICATIONS **2,501** CITATIONS
SEE PROFILE

Gordon Roberts
University of Leicester
317 PUBLICATIONS **9,826** CITATIONS
SEE PROFILE

James Feeney
MRC National Institute for Medical Research
315 PUBLICATIONS **7,804** CITATIONS
SEE PROFILE

J. Mol. Biol. (1998) **277**, 119–134

JMB

The Solution Structure of the Complex of *Lactobacillus casei* Dihydrofolate Reductase with Methotrexate

Angelo R. Gargaro[1], Alice Soteriou[1], Thomas A. Frenkiel[2] Christopher J. Bauer[2], Berry Birdsall[1], Vladimir I. Polshakov[3] Igor L. Barsukov[4], Gordon C. K. Roberts[4] and James Feeney[1]*

[1]*Division of Molecular Structure and* [2]*MRC Biomedical NMR Centre National Institute for Medical Research, The Ridgeway Mill Hill, London NW7 1AA UK*

[3]*Center for Drug Chemistry Moscow 119815, Russia*

[4]*Department of Biochemistry University of Leicester P.O. Box 138, Medical Sciences Building, University Road Leicester LE1 9HN, UK*

**Corresponding author*

We have determined the three-dimensional solution structure of the complex of *Lactobacillus casei* dihydrofolate reductase (18.3 kDa, 162 amino acid residues) formed with the anticancer drug methotrexate using 2531 distance, 361 dihedral angle and 48 hydrogen bond restraints obtained from analysis of multidimensional NMR spectra. Simulated annealing calculations produced a family of 21 structures fully consistent with the constraints. The structure has four α-helices and eight β-strands with two other regions, comprising residues 11 to 14 and 126 to 127, also interacting with each other in a β-sheet manner. The methotrexate binding site is very well defined and the structure around its glutamate moiety was improved by including restraints reflecting the previously determined specific interactions between the glutamate α-carboxylate group with Arg57 and the γ-carboxylate group with His28. The overall fold of the binary complex in solution is very similar to that observed in the X-ray studies of the ternary complex of *L. casei* dihydrofolate reductase formed with methotrexate and NADPH (the structures of the binary and ternary complexes have a root-mean-square difference over the backbone atoms of 0.97 Å). Thus no major conformational change takes place when NADPH binds to the binary complex. In the binary complex, the loop comprising residues 9 to 23 which forms part of the active site has been shown to be in the ''closed'' conformation as defined by M. R. Sawaya & J. Kraut, who considered the corresponding loops in crystal structures of complexes of dihydrofolate reductases from several organisms. Thus the absence of the NADPH does not result in the ''occluded'' form of the loop as seen in crystal studies of some other dihydrofolate reductases in the absence of coenzyme. Some regions of the structure in the binary complex which form interaction sites for NADPH are less well defined than other regions. However, in general terms, the NADPH binding site appears to be essentially pre-formed in the binary complex. This may contribute to the tighter binding of coenzyme in the presence of methotrexate.

Keywords: NMR; DHFR; methotrexate; NADPH; structure

Present address: A. Soteriou, Department of Chemistry, University of Edinburgh, Edinburgh, UK.

Abbreviations used: COSY, correlated spectroscopy; DANTE, delays alternating with nutation for tailored excitation; DHFR, dihydrofolate reductase; DSS, sodium-2,2-dimethyl-2-silapentane-5-sulphonate; DQF, double quantum filtered; GARP-1, globally optimised alternating phase rectangular pulse; HNHA, 3D experiment correlating amide NH and α-CH protons; HNHB, 3D experiment correlating amide NH and β-CH protons; HSQC, heteronuclear single quantum coherence; MTX, methotrexate; NMR, nuclear magnetic resonance; NOE, nuclear Overhauser effect; NOESY, nuclear Overhauser effect spectroscopy; r.m.s., root-mean-square; ROESY, rotating frame Overhauser effect spectroscopy; SCUBA, stimulated cross-peaks under bleached alphas; S_{rep}, representative structure; TOCSY, total correlation spectroscopy; TSP, 3-(trimethysilyl) propionic acid Na salt; 4D, four-dimensional; 3D, three-dimensional; 2D, two-dimensional; 1D, one-dimensional.

0022–2836/98/110119–16 $25.00/0/mb971560

Introduction

Dihydrofolate reductase (DHFR; EC 1.5.1.3) catalyses the NADPH-dependent reduction of 7,8-dihydrofolate to 5,6,7,8,-tetrahydrofolate which is an important intermediate in the synthesis of serine, methionine and thymidylic acid (Blakley, 1985). The enzyme is of considerable pharmacological interest being the target of a number of ''antifolate'' drugs such as methotrexate (MTX, an antineoplastic agent (see Figure 1)), trimethoprim (an antibacterial agent) and pyrimethamine (an antimalarial agent). Such drugs act by inhibiting the enzyme in parasitic or malignant cells. There have been several studies aimed at investigating the specificity of the ligand binding (see for example Roth & Cheng, 1982; Baccanari & Kuyper, 1993) and extensive structural information has been obtained on a number of DHFR complexes from different species using NMR and X-ray crystallography (reviewed by Blakley, 1985; Freisheim & Matthews, 1984; Feeney, 1990, 1996; Feeney & Birdsall, 1993). For the enzyme from *Escherichia coli*, there are high-resolution crystal structures available on the enzyme alone (Bystroff & Kraut, 1991) several binary complexes (Bolin *et al*., 1982; Kuyper *et al*., 1982; Matthews *et al*., 1985a,b; Bystroff *et al*., 1990; Warren *et al*., 1991; Reyes *et al*., 1995; Lee *et al*., 1996; Sawaya & Kraut, 1997) and ternary complexes (Bystroff *et al*., 1990; Sawaya & Kraut, 1997). X-ray structures have also been reported for complexes formed with the human (Oefner *et al*., 1988; Davies *et al*., 1990; Lewis *et al*., 1995), chicken liver (Matthews *et al*., 1995a,b; McTigue *et al*., 1993), *Pneumocystis carinii* (Champness *et al*., 1994), *Staphylococcus aureus* (Dale *et al*., 1997) and *Lactobacillus casei* (Bolin *et al*., 1982; Filman *et al*., 1982; Matthews *et al*., 1985b) enzymes. There has been a great deal of interest in monitoring loop and subdomain movements in dihydrofolate reductases, since several of these are believed to be functionally important. Defining loop structures on the outside of proteins is difficult in crystal studies because of the possible structural perturbations from crystal packing forces. The most thorough investigations to date have been made by Sawaya & Kraut (1997) who addressed this problem by comparing different complexes crystallised in the same space group. However, it is clearly important to define the structure and mobility of the important surface loops in solution.

Several groups have published NMR signal assignments of complexes of the *Lactobacillus casei*

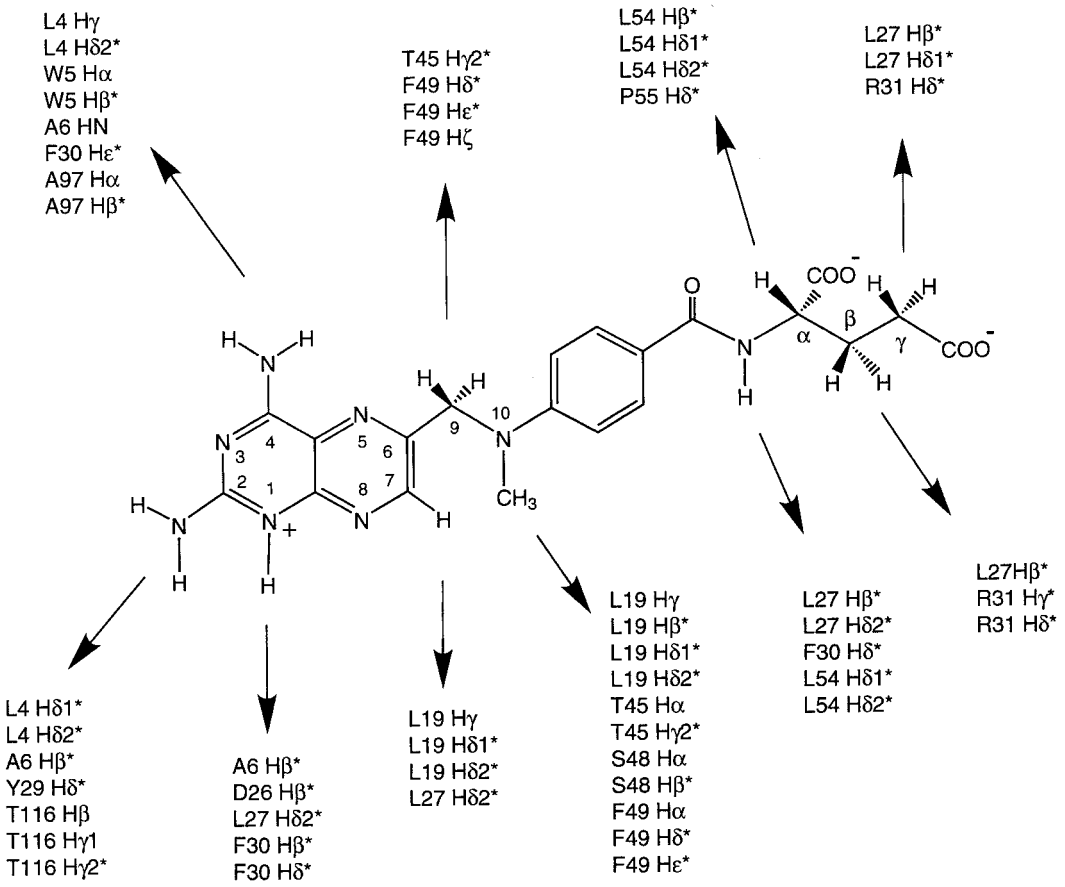

Figure 1. Molecular structure of methotrexate. The methotrexate dihedral angles χ_1 and χ_2 referred to in the test correspond to the N-C^{α}-C^{β}-C^{γ} and C^{α}-C^{β}-C^{γ}-C^{δ} torsion angles, respectively. The NOEs detected between methotrexate and protein protons in the *L. casei* dihydrofolate reductase-methotrexate complex are indicated on the structure.

(Carr *et al.*, 1991; Soteriou *et al.*, 1993), *E. coli* (Falzone *et al.*, 1994), *S. aureus* (Altmann *et al.*, 1997) and human (Stockman *et al.*, 1992) enzymes. However, the only structures of DHFR complexes in solution reported to date have been obtained by using NOE-based distance restraints to dock ligands into the protein using X-ray structural data from a related complex as a starting point (Martorell *et al.*, 1994; Morgan *et al.*, 1995; Johnson *et al.*, 1997). As yet there has been no complete structure determination of a DHFR complex in solution using NMR methods. Previous NMR studies have included determinations of binding sites and charged states of interacting groups in the complex (Cocco *et al.*, 1983; Antonjuk *et al.*, 1984; Birdsall *et al.*, 1981, 1984, 1997; Bevan *et al.*, 1985; Searle *et al.*, 1988; Gerothanassis *et al.*, 1996; Gargaro *et al.*, 1996; Nieto *et al.*, 1997), studies of dynamic processes in the bound ligands and their interacting groups on the protein (Searle *et al.*, 1988; Birdsall *et al.*, 1989a; Nieto *et al.*, 1997) and characterisations of multiple conformations in several complexes (Gronenborn *et al.*, 1981; Birdsall *et al.*, 1982, 1989b, 1990).

Many of these earlier NMR studies relied on using a combination of NMR results and X-ray structural data and hence assumed that the solution and crystal structures were similar. This assumption was supported by early NMR studies on DHFR which showed that the same elements of secondary structure are present in the solution and the crystal states (Carr *et al.*, 1991). Further support for the assumption came when all the early signal assignments made by correlating NOE information with distances obtained from X-ray structures were shown to be correct when they were subsequently compared with assignments based only on NMR information (Carr *et al.*, 1991; Soteriou *et al.*, 1993). While these indications of similarity between the solution and crystal structures are encouraging, it is clearly important to determine the actual structures of DHFR-ligand complexes in solution since such structures will provide a more secure basis for investigating the specificities of ligand binding in solution.

Here, we report the first complete structure determination of a DHFR complex, *L. casei* DHFR-MTX, using only NMR methods. This complex was chosen as the first complex to study because it gave high quality spectra and its solution structure would allow us to make comparisons with the X-ray structure of the ternary complex *L. casei* DHFR-MTX-NADPH (Bolin *et al.*, 1982) which is the only available X-ray structure for an *L. casei* DHFR complex. It also provides a reference structure for making comparisons with solution structures of other inhibitor complexes with *L. casei* DHFR currently being investigated to gain insights into the origins of ligand binding specificity; these include the binary complexes of DHFR with trimethoprim and trimetrexate, and ternary complexes involving these ligands together with NADPH or $NADP^+$. The solution structure will also help in interpreting NMR data from related complexes where the full structure has not yet been determined. Until now, our ligand docking studies in solution have had to use the X-ray structure of the ternary DHFR-methotrexate-NADPH complex as a starting structure. The solution structure reported here provides a more appropriate starting structure for use in such ligand docking studies. Finally, the availability of solution structures of protein complexes will allow us to define the structures of loops on the outside of the protein and to compare their structures in different complexes unperturbed by crystal packing forces. In particular, we have examined the conformation of the loop comprising residues 9 to 23 (*L. casei* numbering) that forms part of the active site. This loop has been extensively studied in crystals where it appears to adopt different conformations in different crystalline complexes (Sawaya & Kraut, 1997).

Results and Discussion

Signal assignments and NMR-determined restraints

Many of the ^1H, ^{15}N and ^{13}C signal assignments for the DHFR-methotrexate complex have been reported previously (Carr *et al.*, 1991; Soteriou *et al.*, 1993). These have now been further extended to include the assignments from Arg9, Arg31, Gln33, Lys37 and Pro53 and exchangeable protons from the guanidino groups of arginine residues and also many stereospecific assignments. More than 99% of the non-exchangeable protons have been assigned and a complete list of the assignments is provided as supplementary material. The distance restraints were obtained from NOE measurements and the dihedral angle constraints from coupling constant and NOE data as described in Materials and Methods. The complete structure calculations were carried out using a final restraint list containing 2531 distance restraints, 361 dihedral angle restraints and 48 hydrogen bond restraints (the experimental constraints have been deposited with the Brookhaven Protein Data Bank; see Materials and Methods). The extensive list of intermolecular NOEs between the methotrexate and the protein protons is summarised in Figure 1. From an analysis of the final 21 converged structures (see Figure 2) using PROMOTIF (Hutchinson & Thornton, 1996) a consensus secondary structure was identified for the NMR ensemble. A representative structure S_{rep} was selected from the ensemble of calculated structures as being the one which is closest to the average structure (Sutcliffe, 1993; Figure 3). The overall covalent geometry in the family of 21 structures is good (Table 1) and there are no residues in disallowed regions of the Ramachandran plot (Figure 4). Superposition of the calculated structures (Figure 2) shows that the protein is well defined with a root-mean-square (r.m.s.) deviation about the average structure of 0.46 Å for the backbone atoms (C, C^α and N) and

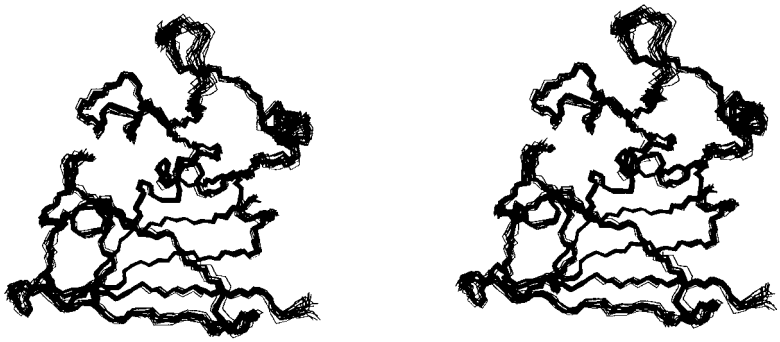

Figure 2. Stereoview of a superposition over the backbone atoms (C, C^{α} and N) of residues 1 to 162 of the final 21 structures of the *L. casei* dihydrofolate reductase-methotrexate complex. The superpositions were made onto the backbone atoms of the representative structure, S_{rep}.

0.82 Å for all heavy atoms (see Table 1). A plot of the r.m.s. differences of the backbone atoms against the amino acid sequence (Figure 5) indicates that although all parts of the protein are well defined, the regions containing residues 16 to 18 and 64 to 72 are somewhat less well defined. In *L. casei* DHFR, the N and C termini are buried so that there are no long unstructured tails.

The solution structure of the DHFR-methotrexate complex

From the observed NOEs and amide proton exchange data (Carr *et al.*, 1991), and the PROMOTIF analysis of the family of NMR structures, it is obvious that a large proportion of the secondary structural elements present in DHFR are β-sheet in nature. Examination of Figure 3 and the PROMOTIF output indicates that the structure has a twisted β-sheet formed from eight β-strands (residues 2 to 7 (A), 38 to 41 (B), 58 to 62 (C), 74 to 76 (D), 94 to 98 (E), 112 to 118 (F), 136 to 144 (G) and 153 to 160 (H); seven parallel (A to G) and one antiparallel (H) (nomenclature of Bolin *et al.*, 1982)). There are four α-helices (residues 24 to 32 (B), 43 to 48 (C), 79 to 88 (E) and 100 to 105 (F)) packed against the twisted β-sheet with two helices on each side of the sheet. The structure includes several β-α-β motifs as previously described (Carr *et al.*, 1991). In 50% of the structures there are two other regions which interact with each other in a β-sheet manner, one within the 9 to 23 loop (residues 11 to 14) and the other in the F to G loop (residues 126 to 127). These additional short β-strands will be considered later in the context of the movements of the 9 to 23 loop which determine the ''open'', ''closed'' and ''occluded'' forms of the binding site discussed by Sawaya & Kraut (1997).

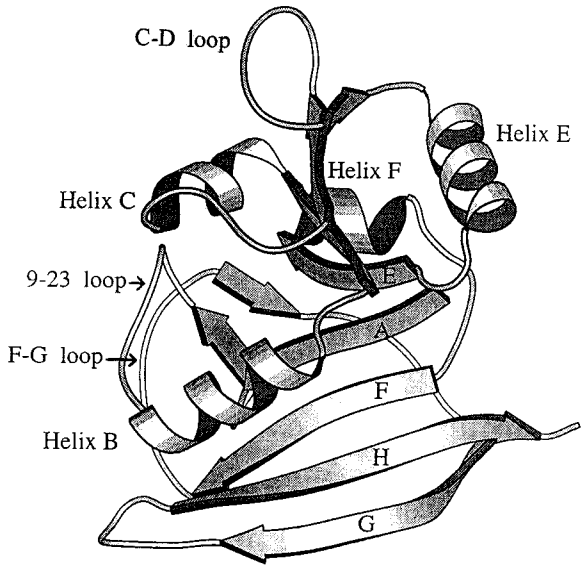

Figure 3. MOLSCRIPT representation (Kraulis, 1991) of the representative structure, S_{rep}, of the *L. casei* dihydrofolate reductase-methotrexate complex showing the elements of secondary structure.

Evidence for helix capping (Presta & Rose, 1988) of helix B is found in the structures. In the majority of the initial structures (see Materials and Methods) calculated with no hydrogen bond constraints, the γ-hydroxyl proton of Thr34 is close to the carbonyl oxygen atom of Phe30. A signal has also been detected for the γ-hydroxyl proton of Thr34 which supports its involvement in a strong hydrogen bond. This interaction of the threonine residue hydroxyl proton with the phenylalanine residue carbonyl group would cap helix B. In the crystal structure of the ternary complex, these atoms are also close enough to form a hydrogen bond (Bolin *et al.*, 1982).

Figure 6(a) shows the pteridine binding site for the 21 NMR-determined structures. This shows that the side-chains of residues interacting with the pteridine ring are well determined. The ^{13}C chemical shifts of the C2 carbon of bound methotrexate measured as a function of pH had previously indicated that the N1 position is protonated and that its p*K* value is increased by at least two units (Cocco *et al.*, 1981; Cheung *et al.*, 1993) in the DHFR-MTX complex. The methotrexate N1 proton is detected at a chemical shift of 16.85 ppm, and was assigned by its intramolecular NOEs. The detection of this proton and the modified pK_a value for the N1 position in the bound methotrexate strongly suggest that this proton is involved in a hydrogen-bonding interaction with a charged group on the protein. In the family of initial structures, the only nearby charged group acceptor (less than 4 Å away) is the carboxylate group of Asp26, with the next closest being more than 8 Å away. Thus the methotrexate N1 proton

Table 1. NMR restraints and structural statistics for the DHFR-methotrexate complex

A. Restraints used in the final structure calculation		
NOEs:		
Long-range ($\|i-j\|>4$)	976	
Medium-range ($1<\|i-j\|\leqslant 4$)	376	
Sequential ($\|i-j\|=1$)	583	
Intraresidue	536	
Protein-ligand	54	
Ligand-ligand	6	
Dihedral angles:		
Phi (ϕ)	131	
Psi (ψ)	128	
Chi-1 (χ_1)	95	
Chi-2 (χ_2)	6	
Chi-3 (χ_3)	1	
MTX	3	
B. Constraint violations in the final ensemble of 21 structures		
Number of NOE constraint violations above 0.2 Å	0	
Number of dihedral angle violations above 5°	0	
XPLOR energies (kcal mol^{-1})[a]		
	⟨S⟩[b]	S_{rep}
E_{CDIH}	0.045 ± 0.016	0.039
E_{NOE}	0.149 ± 0.119	0.142
C. Deviations from idealised geometry		
	⟨S⟩	S_{rep}
Bonds (Å) $\times 10^3$	3.84 ± 0.03	3.83
Angles (°)	0.316 ± 0.004	0.314
Impropers (°)	0.150 ± 0.002	0.152
D. Structural statistics for final ensemble		
PROCHECK analysis:		
	⟨S⟩	S_{rep}
% of residues in most favourable region of Ramachandran plot	78	78
E. Atomic r.m.s. differences (Å)		
	Backbone atoms (C, C^{α} and N)	Heavy atoms
Residues 1 to 162[c]	0.46 ± 0.07	0.82 ± 0.05
X-ray *versus* NMR	0.97 ± 0.07	3.19 ± 0.02[d]

[a] The force constant used to calculate E_{NOE} was 50 kcal mol^{-1} $Å^2$. The force constant used to calculate E_{CDIH} was 200 kcal mol^{-1} rad^{-2}.
[b] ⟨S⟩ is the ensemble of 21 final structures, S_{rep} is the representative structure (see the text).
[c] For the NMR structures these numbers refer to the mean structure.
[d] Residues 8, 10, 51 and 89 were excluded from this calculation due to sequence differences and missing density in the X-ray structure.

is interacting with the carboxylate group of Asp26. PM3 SCF MO (self consistent field molecular orbital) quantum mechanical calculations of the interactions between the 2,4-diaminopyrimidine moiety and aspartic acid residue in the active site of the protein indicated that the aspartic acid carboxylate group would interact with the N1 proton and a proton in the nearby 2-NH_2 group (Polshakov *et al*., 1995a). The γ-hydroxyl proton of Thr116 is also observed in the NMR spectra of the complex in H_2O suggesting that it is involved in a hydrogen-bonding interaction with its nearest neighbour, namely Asp26. The interaction of Asp26 and Thr116 with the N1H and the 2-NH_2 of the pteridine ring can be seen in Figure 6(a). This pattern of hydrogen bonding is identical with that seen in the crystal structure (Bolin *et al*., 1982).

In the solution structure of the binary complex the L-glutamate α- and γ-carboxylate groups of methotrexate interact with the Arg57 guanidino group and the His28 imidazole group, respectively. These interactions were detected in our earlier NMR studies (Antonjuk *et al*., 1984; Gargaro *et al*., 1996) and in the X-ray work of Bolin *et al*. (1982). Recently we used $^{15}N/^{1}H$ HSQC spectra to characterise the interaction between the guanidino group of Arg57 and methotrexate (Gargaro *et al*., 1996; Nieto *et al*., 1997) and showed that there was a symmetrical end-on interaction of a ligand carboxylate group with the two ''inner'' NH^{η} guanidino protons ($NH^{\eta}12$ and $NH^{\eta}22$). However, we were unable to say if the interaction involved the α- or the γ-carboxylate group. Ligand-protein NOEs used to determine the initial solution structures showed unequivocally that the α-carboxylate group of methotrexate interacts with Arg57. Although the values of the torsion angles in the L-glutamate part of the ligand are similar in the binary and ternary complexes, the χ_1 angle is not well defined in the solution structure of the binary

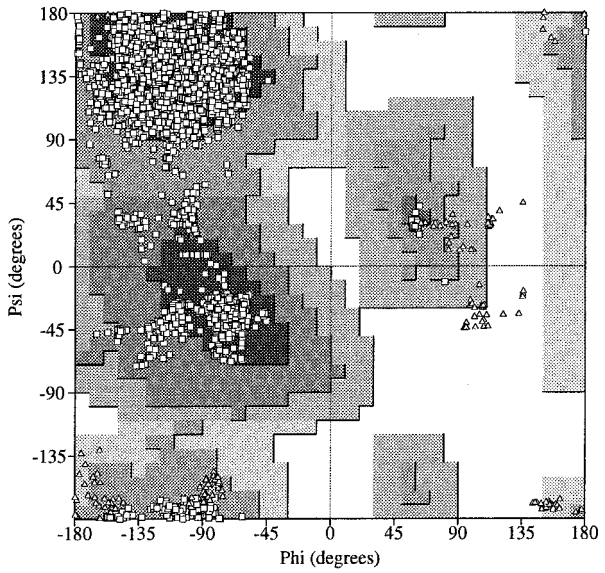

Figure 4. A Ramachandran plot of the ϕ and ψ torsion angles for all residues of the 21 final structures of the *L. casei* dihydrofolate reductase-methotrexate complex generated with PROCHECK-NMR (Laskowski *et al.*, 1996). Triangles represent Gly and Pro residues and squares represent all other residues. The background of the plot is shaded according to the probability of observing non-Gly and non-Pro residues in that locality in a high-resolution crystal structure; the most heavily shaded regions are most favoured and the lightest regions are regarded as disallowed.

complex (the observed order parameter, 0.67, presumably reflecting the lack of restraints and stereospecific assignments for the β-protons of the L-glutamate moiety). The relative orientation of the carboxylate groups in the L-glutamate moiety of methotrexate was confirmed by observation of protein-ligand NOEs involving the L-glutamate side-chain protons which fix the χ_2 angle of methotrexate at −180° in the majority of the calculated NMR solution structures, with an order parameter of 0.87. The interactions involving the methotrexate carboxylate groups and the Arg57 and His28 resi-

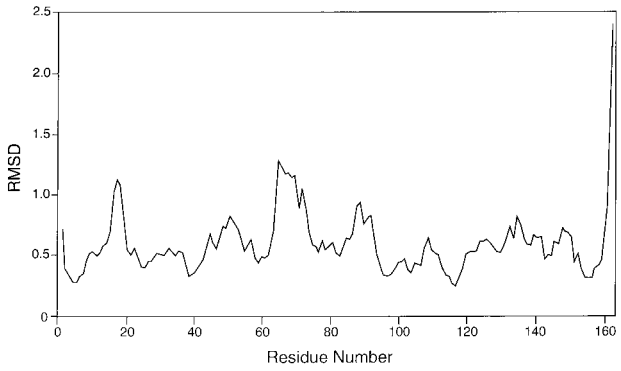

Figure 5. Plot of the local three residue average r.m.s. difference (RMSD) over the backbone atoms (C, C^{α} and N) against the amino acid sequence.

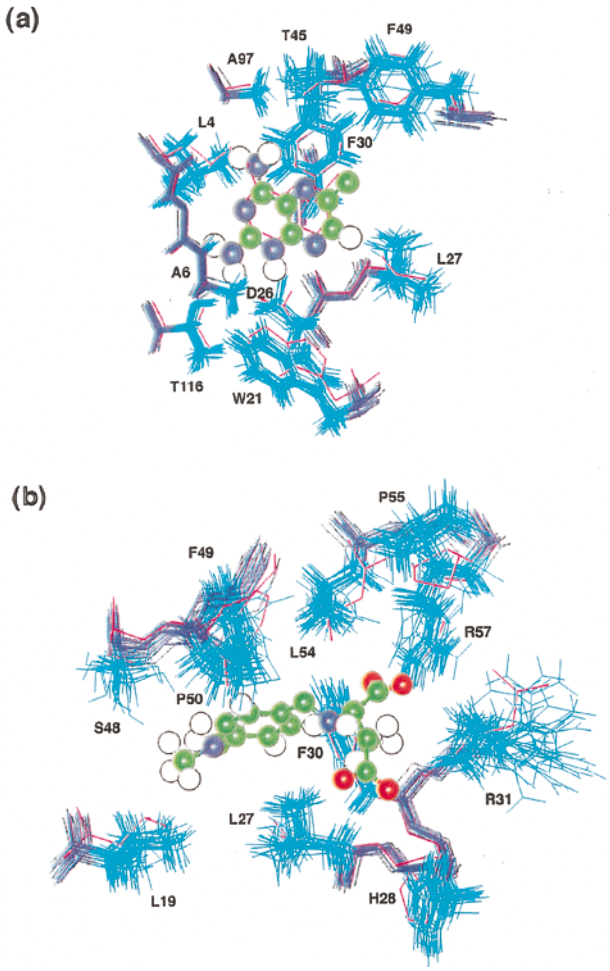

Figure 6. Superposition of the 21 NMR-determined solution structures (backbone in dark blue and side-chains in light blue) for residues in the binding site of methotrexate in the *L. casei* dihydrofolate reductase-methotrexate complex. (a) The environment of the pteridine ring moiety, and (b) the environment of the para-amino benzoyl-L-glutamate moiety. The superposition of the backbone atoms (C, C^{α} and N) of residues 1 to 162 of the final 21 structures of the *L. casei* reductase-methotrexate complex was made onto the backbone atoms of the representative structure, S_{rep}. The crystal structure of the ternary complex (shown in magenta) was superimposed on the S_{rep} structure in the same way. The methotrexate from the S_{rep} structure is shown in ball and stick representation.

dues can be seen in Figure 6(b) which shows the 21 NMR-determined structures around the binding site of the *p*-amino-benzoyl-L-glutamate moiety.

Comparison with the X-ray structure of the *L. casei* DHFR-methotrexate-NADPH complex

The overall fold in the binary DHFR-MTX NMR-determined structure is very similar to that observed in the crystal structure of the ternary DHFR-MTX-NADPH complex (Bolin *et al.*, 1982; Filman *et al.*, 1982) with a r.m.s. difference over

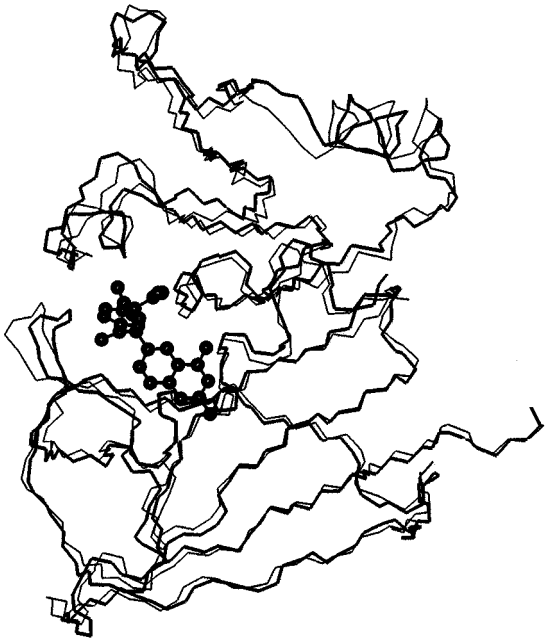

Figure 7. Superposition of the NMR-determined solution structure for the *L. casei* dihydrofolate reductase-methotrexate complex (the S_{rep} structure) on the crystal structure of the ternary complex of *L. casei* dihydrofolate reductase-methotrexate-NADPH (from Bolin *et al*., 1982). The superposition was made using the backbone atoms (C, C^{α} and N) of all 162 residues. The solution structure of the binary complex is displayed in thicker lines and includes the methotrexate structure shown in ball and stick representation.

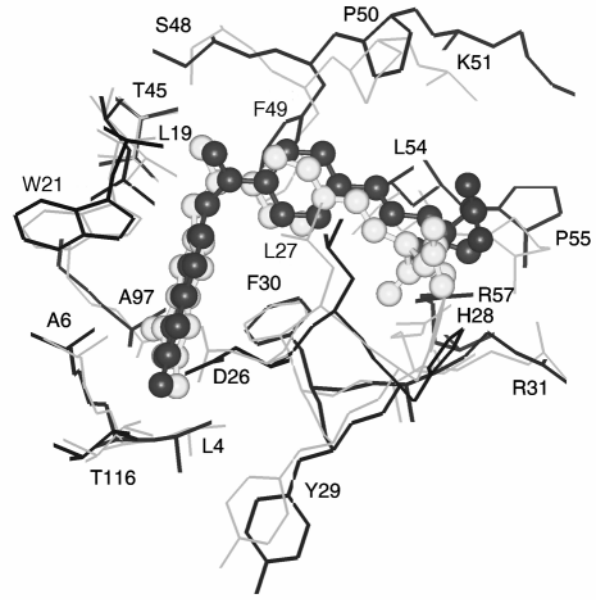

Figure 8. A comparison of the methotrexate binding site in the S_{rep} NMR-determined solution structure (dark shading) of the *L. casei* dihydrofolate reductase-methotrexate complex and the crystal structure (light shading) of the ternary complex. The superposition of structures was made over the backbone atoms (C, C^{α} and N) of all 162 residues in the two structures.

the backbone atoms of 0.97 Å (see Table 1 and Figure 7). The bound methotrexate was found to occupy a similar position in the binary and ternary complexes as shown in Figure 8. Thus, no major conformational change takes place in the protein when NADPH binds to the binary DHFR-methotrexate complex. A similar conclusion was reached by comparing crystal structures of the binary DHFR-MTX complex from *E. coli* and the ternary DHFR-MTX-NADPH complex of *L. casei* (Bolin *et al*., 1982).

A PROMOTIF analysis of the binary and ternary structures indicates that strand E is two residues longer in the binary complex (94 to 98 rather than 96 to 98). The PROMOTIF analysis additionally identified the two additional elements of β-sheet (residues 12 to 14 and 126 to 127) mentioned earlier; these are also seen in the PROMOTIF analysis of the ternary complex. The four α-helices identified by PROMOTIF are identical in the binary and ternary structures. In our earlier work (Carr *et al*., 1991) it was suggested that helix B was one turn shorter in the binary complex but, with the more complete set of assignments now available, we find that this is not the case.

With regard to the coenzyme binding site it is noted that the loop comprising residues 64 to 72 (between β-strands C and D, see Figure 3) appears to be less well defined than other loops in the structure of the binary complex. However, it is noted that the *B*-factors of atoms in the corresponding loop in the ternary complex (Bolin *et al*., 1982) are also generally large than those for other loops, and Epstein *et al*. (1995) have reported lower than average order parameters for residues 67 and 69 of the *E. coli* enzyme in its complex with folate. Several residues in this region make contacts with NADPH in the crystal structure of the ternary complex and it has recently been suggested that this loop may play a role in the negative cooperativity between NADPH and tetrahydrofolate binding (Basran *et al*., 1997).

A detailed analysis of the solution and crystal structures shows that although the main differences occur around the NADPH binding site (for example, the backbone atoms of residues in the sequence His77 to Val79 in the binary complex are displaced by about 2 Å from their positions in the ternary complex) the main characteristic features of the NADPH binding site are essentially present in the binary complex. This is seen particularly clearly for the nicotinamide ring binding site given in Figure 9(a). This shows the structure of the residues that are known from the crystal structure to interact with the reduced nicotinamide mononucleotide moiety of NADPH, together with the 21 NMR solution structures from the binary DHFR-methotrexate complex where there is no NADPH present. The positions of the backbone and side-chain atoms are seen to be well determined, and

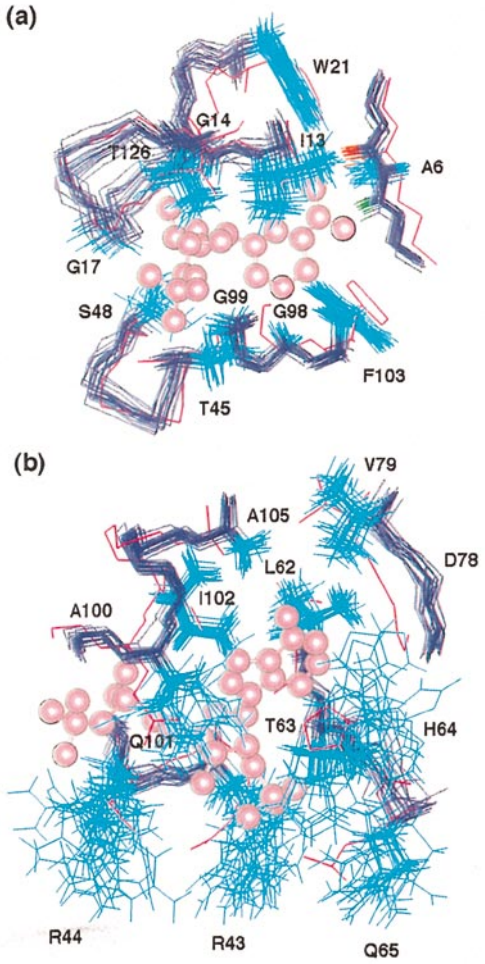

Figure 9. Superposition of the 21 NMR-determined solution structures (backbone in dark blue and side-chains in light blue) for residues in the unoccupied binding site of NADPH in the *L. casei* dihydrofolate reductase-methotrexate binary complex, (a) in the environment of nicotinamide mononucleotide moiety, showing the Ala6 NH proton in green and its carbonyl O in red, and (b) in the environment of the adenosine moiety of NADPH. The superposition of the backbone atoms (C, C^{α} and N) of residues 1 to 162 of the final 21 structures of the *L. casei* dihydrofolate reductase-methotrexate complex was made onto the backbone atoms of the representative structure, S_{rep}. The crystal structure of the ternary complex (shown in magenta) was superimposed on the S_{rep} structure using the backbone atoms (C, C^{α} and N) of all 162 residues. The coenzyme (from the crystal structure of the ternary complex) is shown in ball and stick representation occupying the pre-formed binding site in the binary complex.

there is an appropriate space available for the coenzyme to occupy. The Ala6 backbone oxygen atom and its NH group are ideally positioned to form the two hydrogen-bonding interactions with the nicotinamide amide group as seen previously in the crystal structure of the ternary complex (Filman *et al.*, 1982). The turn involving the conserved residues Gly98 and Gly99 also has a very similar structure in the binary and ternary complex including a *cis* peptide bond. Figure 9(b) shows the environment around the vacant adenosine binding site. It is seen that while some of the residues have well-ordered structures (Leu62, Val79, I102 and Ala105), the side-chains for other residues are not well defined in the NMR solution structures (Arg43, Arg44, Thr63, His64, Gln65 and Gln101). To assess whether or not there is sufficient space to accommodate this part of NADPH within the NMR structures we have analysed the possible unfavourable steric interactions between protein and coenzyme by using the BUMP routine within Insight. We have examined all 21 NMR structures with the superposed NADPH from the crystal structure (in this case, the superposition of the crystal structure was carried out using only the backbone atoms (C, C^{α} and N) of residues around the coenzyme binding site (5 to 7, 13 to 21, 42 to 48, 62 to 65, 77 to 79 and 98 to 105)). Most of the unfavourable steric interactions identified could easily be removed by changing the conformation of the side-chains. For example, in several of the structures there is an unfavourable steric interaction involving the γ-CH of Leu62. In fact, the χ_1 of Leu62 is 180° in the binary complex and −60° in the ternary complex. Similarly there are some structures in which there are unfavourable interactions with the side-chains of Arg43, Arg44, Thr63 and Gln101 (these are not well defined in the solution structure; their side-chains are essentially disordered as judged by their dihedral angle order parameters). These side-chains are all expected to make direct interactions with the coenzyme in the ternary complex and such interactions could be made by selecting out the appropriate side-chain conformations. The BUMPS calculations indicated that there are some unfavourable steric interactions involving protein backbone atoms and the coenzyme. These mainly involve residues Gly17, Gly99 and Ala100, but fairly modest movements in the backbone (around 0.5 Å) would be sufficient to make the pre-formed site fully accessible to NADPH. Gly17 is part of the 9 to 23 loop which has been detected in different conformations in different complexes in the crystal state (Sawaya & Kraut, 1997). This loop will be discussed in more detail below.

Active site loop conformations

Sawaya & Kraut (1997) have examined an extensive series of binary and ternary complexes of *E. coli* dihydrofolate reductase formed with various ligands and they noted that the loop comprising residues 10 to 24 (loop 9 to 23 in *L. casei* DHFR) can exist in various conformations in the different complexes. They detected three possible conformations of the loop which they described as ''open'', ''closed'' or ''occluded'' forms with respect to the active site. A fourth possibility with the loop in a disordered state was also noted. The open form is the one most frequently observed in the crystal studies and in this form the loop extends

outside its position in the closed and occluded structures (it is not an intermediate form between the latter structures). The closed form loop extends across the active site with the residues at the centre of the loop (16 to 19 in *E. coli* DHFR, corresponding to residues Lys15 to His18 in *L. casei* DHFR) forming a short antiparallel β-sheet and a hairpin turn which effectively seals the active site by forming a hydrogen bond between the Asn18 (Hδ21) in the hairpin and the His45(O) in helix C. Further pairs of hydrogen bonds are formed between residues on this loop and residues on the loop between the F and G β-strands (Gly15(O) to Asp122(HN) and Glu17(HN) to Asp122(Oδ2)). In this closed conformation, residues in the loop also interact with the coenzyme nicotinamide-ribose moiety in crystal structures of DHFR complexes containing $NADP^+$. Sawaya & Kraut (1997) noted that the closed form is that seen in the crystal structure of the ternary complex of *L. casei* DHFR with methotrexate and NADPH (Bolin *et al*., 1982) and in all DHFR structures so far reported from sources other than *E. coli*. In the occluded conformation, the loop occupies part of the NADPH binding site and has a 3_{10} helix instead of the β-sheet/hairpin. Sawaya & Kraut (1997) suggested that, in some crystal studies, the occluded form sometimes appears to be destabilised by crystal packing forces.

A comparison of the solution structure of the corresponding loop (9 to 23) in the binary *L. casei* DHFR-methotrexate complex with the structure of the closed, open and occluded forms in the loop found in X-ray structures of other complexes (see Figure 10) indicates that in the *L. casei* DHFR-methotrexate complex, the 9 to 23 loop is present as the closed form in solution. The β-sheet/hairpin is present and the hydrogen bonds between Gly14(O) to Asp125(N) and Asp16(N) to Asp125(Oδ2) exactly parallel the corresponding features seen for the closed form as described by Sawaya & Kraut (1997). In *L. casei* DHFR the residues corresponding to the hydrogen-bonded residues Asn18 and His45 in *E. coli* DHFR are Gly17 and Arg44; even though the latter pair cannot form a hydrogen bond similar to that seen between the *E. coli* residues, the overall similarity of the structure of the 9 to 23 loop in solution to the closed structures seen in other complexes is very clear (see Figure 10). Although there is no coenzyme present in the *L. casei* DHFR-methotrexate complex, the 9 to 23 loop shows no tendency to enter the nicotinamide ring binding pocket and to take up the occluded form. Clearly the closed form can exist in solution even in the absence of coenzyme. Thus there is no need to invoke crystal packing forces as destabilisers of the occluded form in some of the crystal structures where closed forms were observed in complexes with an unoccupied pocket for the nicotinamide ring.

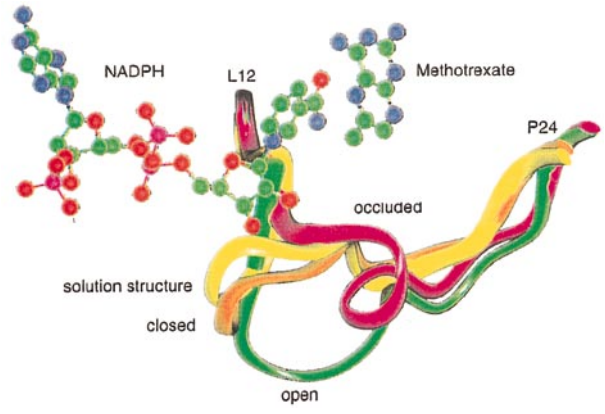

Figure 10. A comparison for several complexes of dihydrofolate reductases of the loop structures corresponding to residues 9 to 23 in *L. casei* dihydrofolate reductase. The structure of the loop in the NMR solution structure of *L. casei* dihydrofolate reductase-methotrexate is labelled solution structure. The other structures (taken from Sawaya & Kraut, 1997) show examples of the closed, open and occluded forms of the loop found in crystal structures of several ligand complexes of *E. coli* dihydrofolate reductase (complexes with NADPH-methotrexate (closed); NADPH (open); 5,10-diazatetrahydrofolate (occluded); Brookhaven PDB codes 1rh3, 1ra1 and 1rx5, respectively).

Conclusions

The comparison of the solution structure of the binary *L. casei* DHFR-methotrexate complex with the crystal structure of the ternary complex DHFR-MTX-NADPH (Bolin *et al*., 1982) indicates that the vacant NADPH binding site in the binary complex is essentially pre-formed for NADPH binding. NADPH binds 700-fold tighter to the enzyme-methotrexate complex than it does to the enzyme alone (Birdsall *et al*., 1980). If there is a difference in conformation or conformational flexibility of the enzyme in the absence of bound ligands, the pre-formed site in the binary complex could contribute in an important way to the much tighter binding observed in the ternary complex. However, a clearer view of the origin of the cooperative binding will only emerge when a solution structure is obtained for enzyme in the absence of ligands where any substantial conformational and flexibility differences between this and the liganded enzymes should become apparent. Three-dimensional structures for the enzyme alone and in its ternary and component binary complexes with coenzyme and substrate analogues will open the way to a more detailed understanding of binding specificity and cooperativity.

Materials and Methods

Preparation of samples

L. casei DHFR was prepared and purified as described previously using an *E. coli* strain into which the structural gene for the *L. casei* enzyme had been cloned (Andrews *et al*., 1985; Dann *et al*., 1976). The *E. coli* cells were grown in minimal media supplemented with

L-tryptophan. DHFR samples were uniformly enriched with ^{15}N and $^{13}C/^{15}N$ by providing [^{15}N]ammonium sulphate (C. K. Gas Products Ltd.) as the sole nitrogen source and [$^{13}C_6$]-D-glucose (C. K. Gas Products Ltd.) as the sole carbon source to the *E. coli* growth medium. Methotrexate was obtained from Sigma Chemicals Co. and the complex with *L. casei* DHFR containing one equivalent of methotrexate was prepared as described (Carr *et al.*, 1991; Soteriou *et al.*, 1993).

NMR experiments

All NMR experiments were performed on Varian UNITY spectrometers operating at proton frequencies of 500 and 600 MHz. The spectra were recorded at 281, 298 or 308 K on either unlabelled, ^{15}N-labelled or $^{13}C/^{15}N$-labelled protein samples at approximately 3 mM concentrations in 500 mM potassium chloride and 50 mM potassium phosphate buffer (pH* 6.5) (pH* values are meter readings uncorrected for deuterium isotope effects).

As most of the assignments for this complex have been described (Carr *et al.*, 1991; Soteriou *et al.*, 1993; Gargaro *et al.*, 1996) we will only discuss, in detail, the experiments recorded to obtained restraints for the structure determination.

2D NOESY (Jeener *et al.*, 1979; Kumar *et al.*, 1981) spectra were recorded in H_2O and ^2H_2O with NOE build-up periods of 50 and 100 ms; ROESY (Bothner-By *et al.*, 1984) spectra were acquired in ^2H_2O with mixing times of 15, 28 and 40 ms, respectively. 1D NOE difference spectra and 2D NOESY spectra recorded at low temperatures (5 and 1°C) were used to detect NOEs from the methotrexate N1 proton (16·85 ppm) to the protein. To identify other ligand-protein NOEs, a $^{12}C/^{13}C$ filtered NOESY (Otting *et al.*, 1986; Otting & Wüthrich, 1990; Fesik *et al.*, 1987) spectrum was acquired with a 100 ms mixing time (see Figure 11). Because unlabelled tryptophan was used in the fermentation (the *E. coli* strain being auxotrophic for tryptophan) this experiment also allowed the identification of NOEs between ring protons of the unlabelled tryptophan and protons on the labelled protein.

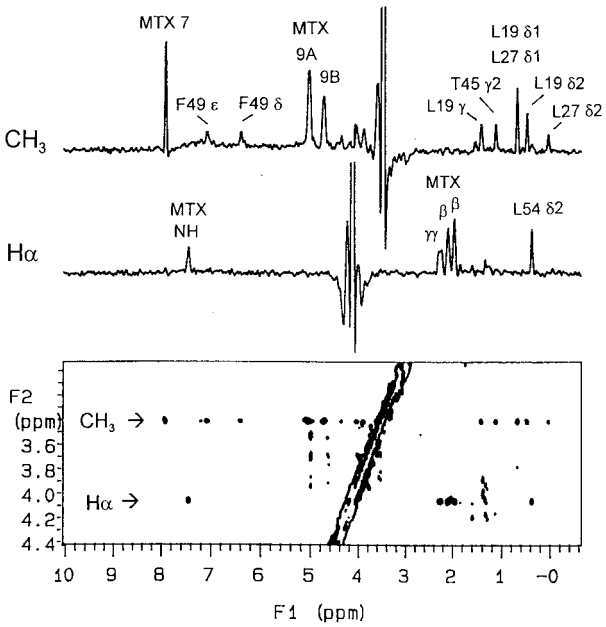

Figure 11. Part of a plot of a $^{12}C/^{13}C$ filtered 2D NOESY spectrum acquired from a sample containing unlabelled methotrexate and ^{13}C-labelled *L. casei* dihydrofolate reductase showing the NOEs involving the methotrexate N10-CH_3 and H^{α} protons.

The following 3D ^{15}N-edited spectra were acquired on the ^{15}N-labelled sample: NOESY-HSQC, using a WATERGATE (Sklenar *et al.*, 1993) version of the original sequence of Marion and co-workers (Marion *et al.*, 1989a,b) with mixing times of 50 ms and 100 ms. Acquisition times were of 23.3 and 24.4 ms in the indirect ^1H dimension, 16 ms in the indirect ^{15}N dimension and 71.1 and 56.6 ms in the real-time ^1H dimension, respectively. The final size of the data matrix was 512 × 128 × 1024 real points in both cases; TOCSY-HSQC (Marion *et al.*, 1989a,b), modified to include WATERGATE solvent suppression, with acquisition times of 22.8, 16 and 71 ms in the indirect ^1H, indirect ^{15}N and real-time ^1H dimensions, respectively, and a mixing time of 52 ms; TOCSY-HMQC (Marion *et al.*, 1989a,b), with a mixing time of 37 ms and a spin-lock power of 6.9 kHz with acquisition times of 9.7, 14.6 and 64 ms in the indirect ^1H, indirect ^{15}N and real-time ^1H dimensions, respectively, to give a final data matrix of 256 × 128 × 1024 real points. The solvent signal was suppressed using a DANTE sequence. The SCUBA technique was used to recover signals of $C^{\alpha}H$ protons near the water resonance (Brown *et al.*, 1988); ROESY-HMQC (Clore *et al.*, 1990), with a spin-lock time of 30 ms, a spin-lock power of 3.7 kHz and acquisition times of 15 ms (indirect ^1H), 11.5 ms (indirect ^{15}N) and 64 ms (real-time ^1H), respectively. Solvent suppression was achieved by using presaturation of the water signal. The final size of the transformed matrix was 256 × 64 × 1024 real points; HNHB (Archer *et al.*, 1991), with a 38 ms delay to allow the evolution of long-range ^1H-^{15}N couplings, was recorded with acquisition times of 10, 13 and 64 ms in the indirect ^1H, indirect ^{15}N and real-time ^1H dimensions, respectively. The final size of the transformed matrix was 256 × 256 × 1024 real points; HNHA (Vuister & Bax, 1993), with acquisition times of 10 ms (indirect ^1H), 28 ms (indirect ^{15}N) and 64 ms (real-time ^1H), respectively. Fourier transformation and zero-filling resulted in a final matrix of 256 × 256 × 1024 real points; HMQC-NOESY-HMQC (Frenkiel *et al.*, 1990; Ikura *et al.*, 1990a) with a NOE build-up period of 100 ms.

Two 3D ^{13}C-edited HMQC-NOESY (Ikura *et al.*, 1990b; Zuiderweg *et al.*, 1990) spectra were acquired with 100 ms mixing times and acquisition times of 10.0 and 9.1 ms in the indirect ^{13}C dimension, 17.6 and 24.0 ms in the indirect ^1H dimension and 56.9 and 68.3 ms in the real-time ^1H dimension, respectively. The position of the ^{13}C carrier frequency was 40.8 ppm in the first experiment and 74 ppm in the second experiment. The second experiment allowed the detection of NOEs between aromatic and aliphatic protons which were obscured by inefficient decoupling of the aromatic signals in the first experiment. After Fourier transformation and zero-filling, the final size of the matrix was 128 × 512 × 1024 real points in both cases.

A 4D $^{13}C/^{13}C$-edited NOESY (Clore *et al.*, 1991; Zuiderweg *et al.*, 1991) spectrum, 100 ms mixing time, was recorded with acquisition times of 5.3, 10.7, 5.3 and 42.7 ms in the ^{13}C, ^1H and ^{13}C indirect dimensions and real-time ^1H dimension, respectively. The spectrum was processed to give a final data matrix of 32 × 256 × 32 × 512 real points. The indirect ^{13}C dimensions were extended by 25% using linear prediction.

The ^{1}H carrier was positioned on the water resonance in all of the experiments. Decoupling during the detection period of the 3D and 4D experiments was achieved using the GARP-1 sequence (Shaka *et al.*, 1985). Phase-sensitive detection in the indirect dimensions was obtained using the method of States and co-workers (States *et al.*, 1982). The spectra were processed and displayed using VNMR (Varian), FELIX (Molecular Simulations Inc.) and in-house software. The 3D and 4D spectra were processed with a 72 degree shifted sine-bell squared window function. The ^{1}H chemical shifts were referenced to DSS (after measuring from dioxane) and the ^{15}N and ^{13}C chemical shifts were referenced to liquid NH_3 and TSP calibrated using the γ ratios method (Live *et al.*, 1984; Wishart *et al.*, 1996).

Distance restraints

The interproton distance restraints were obtained from NOEs measured in the 2D NOESY and ROESY, 3D $^{1}H/^{15}N$ NOESY-HSQC and $^{1}H/^{13}C$ HMQC-NOESY, and 4D $^{13}C/^{13}C$ edited HMQC-NOESY-HMQC spectra. The NOEs were divided into four classes, namely strong, medium, weak and very weak, corresponding initially to distance restraints of 0.0 to 3.0 Å, 0.0 to 4.0 Å, 0.0 to 5.0 Å and 0.0 to 6.0 Å. The last range allows for the inclusion of some spin diffusion effects in the cases where NOEs from 100 ms mixing time NOESY spectra were used (in fact, most of the NOEs were obtained from 50 ms NOESY or ROESY spectra). The lower distance limit was explicitly set to 0.0 Å to achieve improved sampling of conformational space in the initial simulated annealing calculation (Hommel *et al.*, 1992). In the later stages of the calculations a 1.8 Å lower limit was imposed. An r^{-6} sum average, where the r^{-6} distance is weighted by the number of ambiguous NOEs (Nilges, 1995), was used for all non-stereospecifically assigned protons in methylene groups, for protons in methyl groups and the 2′,6′- and 3′,5′-protons in phenylalanine and tyrosine rings. A further correction of 0.5 Å was added to all NOEs involving methyl groups (Clore *et al.*, 1987; Wagner *et al.*, 1987). The number and distribution of NOEs used in the structure calculation is illustrated in Figure 12 and Table 1. The final restraint list contained 2531 NOEs (protein-protein, 976 (long range), 376 (medium range), 583 (sequential) and 536 (intraresidue); protein-ligand, 54; ligand-ligand, six). No intraresidue NOEs between atoms separated by three bonds (e.g. HN-H^{α}, H^{α}-H^{β}) were included in the X-PLOR calculations because these (about 450 NOEs) had already been used for defining the torsion angles in the AngleSearch calculations (Polshakov *et al.*, 1995b). No ambiguous NOEs were included in the calculations.

Torsion angle constraints and stereospecific assignments

Dihedral angle restraints and stereospecific assignments were obtained using the program AngleSearch (Polshakov *et al.*, 1995b). The $^{3}J_{HN,H^{\alpha}}$ coupling constants used in the calculations were measured from HNHA spectra (Vuister & Bax, 1993), the $^{3}J_{N,H^{\beta}}$ and $^{3}J_{N,H^{\alpha}}{}^{i-1}$ were measured from HNHB spectra (Archer *et al.*, 1991) and $^{3}J_{H^{\alpha},H^{\beta}}$ coupling constants were estimated from analysis of 3D $^{1}H/^{15}N$ TOCSY-HMQC spectra recorded with a short mixing time (37 ms) and from splittings in DQF-COSY spectra. The recently corrected Karplus coefficients for $^{3}J_{N,H^{\alpha}}{}^{i-1}$ were used for the estimation of ψ torsion angles (Wang & Bax, 1995). All interatomic distances used in the AngleSearch calculations were estimated from intensities in 3D $^{1}H/^{15}N$ ROESY-HMQC and 2D ROESY spectra (mixing time 30 ms). For residues containing only ϕ, ψ and χ_1 torsion angles, typically six coupling constant parameters and nine distance-related parameters were included in the calculations of torsion angle ranges. No data involving overlapping signals were included in the analysis. A rotamer mixture model was used to analyse rotamer populations in side-chains from surface residues (Polshakov *et al.*, 1995b). The error

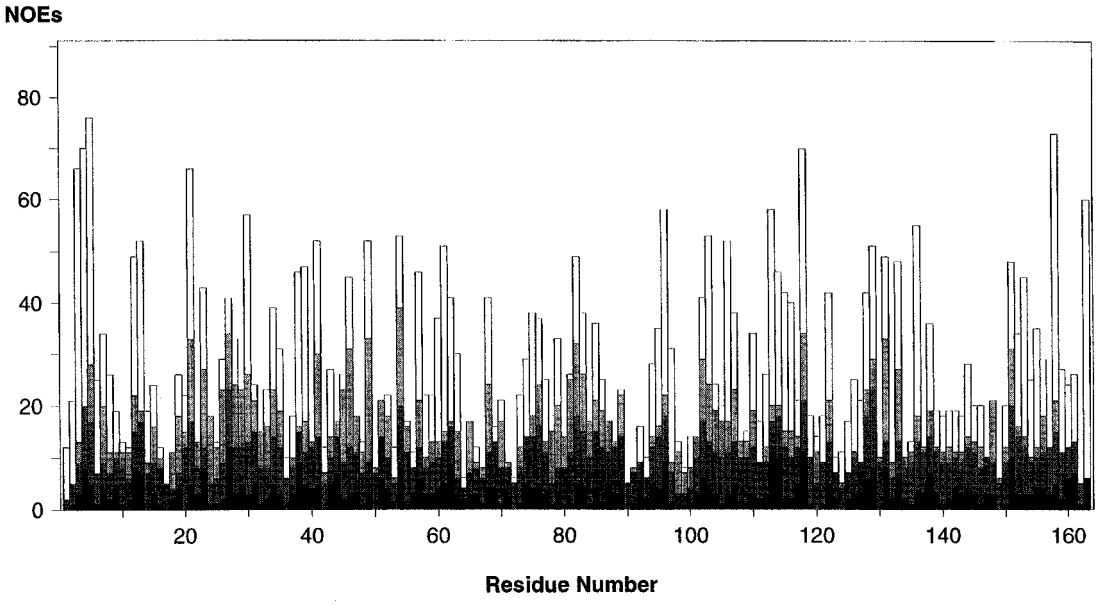

Figure 12. Plot of the distribution of NOEs against amino acid sequence (each NOE is counted twice). NOEs are classified as: intraresidue (black); sequential (dark grey, $(i-j)=1$); medium-range (light-grey, $1<(i-j)\leqslant 4$); and long-range (no shading, $(i-j)>4$).

limits obtained from AngleSearch for the dihedral angles were increased to ±30° for φ, ±50° for ψ and ±40° for χ_1, χ_2 and χ_3, in order to take into account local mobilities and the uncertainties in the Karplus equations used in these studies. The final restraint list contained 361 dihedral angles (φ, 131; ψ, 128; χ_1, 95; χ_2, 6; χ_3, 1).

Hydrogen bond restraints

Hydrogen bond restraints involving backbone NH protons were included in the calculation only after they had been identified in the family of structures using HBPLUS (McDonald & Thornton, 1994) and only where a corresponding slowly exchanging NH proton had been identified in the spectra recorded in ^2H_2O. Two distance restraints were used for each hydrogen bond, 1.7 to 2.5 Å corresponding to the distance between the hydrogen and the acceptor atom and 2.7 to 3.5 Å corresponding to the distance between the donor heavy atom and the acceptor. In total, 41 hydrogen bond restraints involving backbone NH protons were included in the final calculations.

A further seven hydrogen bond restraints involving the ligand and/or residue side-chains were also included and the evidence for these is discussed in Results and Discussion. The only protein-protein hydrogen bond restraints involving side-chains which have been included in the structure calculations are the hydrogen bonds involving Thr116 and Thr34 γ-hydroxyl protons formed with an Asp26 carboxylate oxygen atom and the Phe30 carbonyl oxygen atom, respectively. We also introduced hydrogen bond restraints into the final refinement to mimic the interaction of the α-carboxylate group of methotrexate with Arg57 (Gargaro *et al*., 1996; Nieto *et al*., 1997) and the γ-carboxylate group of methotrexate with His28 Nδ1 (Antonjuk *et al*., 1984; Birdsall *et al*., 1984) as determined previously. Distance restraints involving the methotrexate 1-NH and 2-NH_2 interactions with the Asp26 β-carboxylate oxygen atoms were also included. The final restraint list contained 48 hydrogen bond restraints.

Structure calculations and structure analysis

The structure calculations were performed on Silicon Graphics (Power Indigo^2 and Indy) or Sun (Sparc 10) computers and the calculated structures were visualized using Insight (Molecular Simulations Inc.).

For the complete structure calculation, the final restraint list contained 2531 NOEs, 361 dihedral angles and 48 hydrogen bond restraints. No intramolecular NOEs were included in the calculation where atoms were separated by fewer than three bonds. The three-dimensional structure calculations were performed in an iterative fashion with X-PLOR 3.1 (Brünger, 1992; Brünger *et al*., 1986) using the simulated annealing protocol of Nilges and co-workers (Nilges *et al*., 1988, 1991; Nilges, 1995) with minor modifications. In the first instance, a set of 77 structures was generated using a simulated annealing protocol starting from an extended chain structure for the protein alone (Nilges *et al*., 1991). This involved 120 ps of dynamics at 1000 K followed by cooling to 100 K and finally 400 cycles of conjugate gradient minimization. The ligand was then randomly translated with respect to the N terminus of each of these protein structures and subjected to a simulated annealing calculation similar to that described by Krageland *et al*. (1993). Essentially this involved a 3.0 ps simulated annealing period at 1000 K, followed by cooling to 300 K and restrained molecular dynamics (3.0 ps) then 400 cycles of conjugate gradient minimization. Structures which had no NOE (<0.5 Å) or dihedral angle (<10°) violations after these two protocols were then accepted for further analysis. These initial structures were then used to resolve ambiguities in the NOE data set before being subjected to a slow cooling simulated annealing procedure within X-PLOR with more NOEs and dihedral angle restraints being added in an iterative fashion. The hydrogen bond constraints were only introduced at the very end of refinement. This resulted in a final data set of 21 structures which were selected as having no NOE violations greater than 0.2 Å and no dihedral angle violations greater than 5°. Bond lengths were constrained during the dynamics stages using SHAKE (Ryckaert *et al*., 1977). Parameter and topology files for methotrexate were constructed by using the methotrexate template structure provided with Quanta (Molecular Simulations Inc.) and converting the resulting output files into X-PLOR format. No information about partial charges was used in the calculations. These structures were then compared with the crystal structure of methotrexate tetrahydrate (Sutton *et al*., 1986) and crystal structures of DHFR complexes containing methotrexate to produce a consensus parameter file. The torsion angles for the bonds linking the substituents to the *p*-aminobenzoyl ring were constrained to be within ±50° to the plane of the ring using dihedral angle restraints: in fact it is the NOEs which allow these angles to be well defined.

The analysis of the 21 structures was carried out using X-PLOR 3.1 (Brünger, 1992), PROCHECK-NMR/AQUA (Laskowski *et al*., 1993, 1996), PROMOTIF (Hutchinson & Thornton, 1996), HBPLUS (McDonald & Thornton, 1994) and MolMol (Koradi *et al*., 1996). The analyses showed that there are no residues in disallowed regions of the Ramachandran plot (Figure 4). The structures and NMR-derived constraints have been deposited with the Brookhaven Protein Data Bank (accession number 1AO8).

Acknowledgements

We thank J. E. McCormick and G. Ostler for expert technical assistance, and Dr G. Martorell for assistance with some of the NMR assignments. V.I.P. acknowledges the support of a Howard Hughes International Scholarship. The NMR measurements were made using the facilities at the MRC Biomedical NMR Centre, NIMR, Mill Hill, London.

References

Altmann, S., Labhardt, A. M., Senn, H. & Wüthrich, K. (1997). Sequence-specific ^1H, ^{13}C and ^{15}N assignment of the TMP-resistant dihydrofolate reductase mutant DHFR (F98Y) in the ternary complex with TMP and NADPH. *J. Biomol. NMR*, **9**, 445–446.

Andrews, J., Clore, G. M., Davies, R. W., Gronenborn, A. M., Gronenborn, B., Kalderon, D., Papadopoulos, P. C., Schafer, S., Sims, P. F. G. & Stancombe, R. (1985). Nucleotide sequence of the dihydrofolate reductase gene of methotrexate-resistant *Lactobacillus casei*. *Gene*, **35**, 217–222.

Antonjuk, D. K., Birdsall, B., Burgen, A. S. V., Cheung, H. T. A., Clore, G. M., Feeney, J., Gronenborn, A., Roberts, G. C. K. & Tran, W. (1984). A ^{1}H NMR study of the role of glutamate moiety in the binding of methotrexate to dihydrofolate reductase. *Brit. J. Pharmacol.* **81**, 309–315.

Archer, S. J., Ikura, M., Torchia, D. A. & Bax, A. (1991). An alternative 3D NMR technique for correlating backbone ^{15}N with side chain Hβ resonances in larger proteins. *J. Magn. Reson.* **95**, 636–641.

Baccanari, D. P. & Kuyper, L. F. (1993). Basis of selectivity of antibacterial diaminopyrimidines. *J. Chem. Ther.* **5**, 393–399.

Basran, J., Casarotto, M. G., Basran, A. & Roberts, G. C. K. (1997). Effects of single-residue substitutions on negative cooperativity in ligand binding to dihydrofolate reductase. *Protein Eng.* **10**, 815–826.

Bevan, A. W., Roberts, G. C. K., Feeney, J. & Kuyper, L. (1985). ^{1}H and ^{15}N NMR studies of protonation and hydrogen-bonding in the binding of trimethoprim to dihydrofolate reductase. *Eur. Biophys. J.* **11**, 211–218.

Birdsall, B., Burgen, A. S. V. & Roberts, G. C. K. (1980). Binding of coenzyme analogues to *L. casei* dihydrofolate reductase: binary and ternary complexes. *Biochemistry,* **19**, 3723–3731.

Birdsall, B., Burgen, A. S. V., Hyde, E. I., Roberts, G. C. K. & Feeney, J. (1981). Negative cooperativity between folinic acid and coenzyme in their binding to *L. casei* dihydrofolate reductase. *Biochemistry,* **20**, 7186–7195.

Birdsall, B., Gronenborn, A. M., Hyde, E. I., Clore, G. M., Roberts, G. C. K., Feeney, J. & Burgen, A. S. V. (1982). Hydrogen-1, carbon-13 and phosphorus-31 nuclear magnetic resonance studies of the dihydrofolate reductase–nicotinamide adenine dinucleotide phosphate–folate complex: characterization of three coexisting conformational states. *Biochemistry,* **21**, 5831–5838.

Birdsall, B., Feeney, J., Pascual, C., Roberts, G. C. K., Kompis, I., Then, R. L., Muller, K. & Kroehn, A. (1984). A ^{1}H study of the interactions and conformations of rationally designed brodimoprim analogues in complexes with *Lactobacillus casei* dihydrofolate reductase. *J. Med. Chem.* **23**, 1672–1676.

Birdsall, B., Feeney, J., Tendler, S. J. B., Hammond, S. J. & Roberts, G. C. K. (1989a). Dihydrofolate reductase: multiple conformations and alternative modes of substrate binding. *Biochemistry,* **28**, 2297–2305.

Birdsall, B., Andrews, J., Ostler, G., Tendler, S. J. B., Feeney, J., Roberts, G. C. K., Davies, R. W. & Cheung, H. T. A. (1989b). NMR studies of the differences in the conformations and dynamics of ligand complexes formed with mutant dihydrofolate reductases. *Biochemistry,* **28**, 1353–1362.

Birdsall, B., Tendler, S. J. B., Arnold, J. R. P., Feeney, J., Griffin, R. J., Carr, M. D., Thomas, J. A., Roberts, G. C. K. & Stevens, M. F. G. (1990). NMR studies of multiple conformations in complexes of *L. casei* dihydrofolate reductase with analogues of pyrimethamine. *Biochemistry,* **29**, 9660–9667.

Birdsall, B., Casarotto, M. G., Cheung, H. T. A., Basran, J., Roberts, G. C. K. & Feeney, J. (1997). The influence of aspartate 26 on the tautomeric forms of folate bound to *Lactobacillus casei* dihydrofolate reductase. *FEBS Letters,* **402**, 157–161.

Blakley, R. L. (1985). Dihydrofolate reductase. In *Folates and Pterins* (Blakley, R. L. & Benkovic, S. J., eds), vol. 1, chapt. 5, pp. 191–253, J. Wiley, New York.

Bolin, J. T., Filman, D. J., Matthews, D. A., Hamlin, R. C. & Kraut, J. (1982). Crystal structures of *E. coli* and *L. casei* dihydrofolate reductase refined to 1.7 Å resolution. I. General features and binding of methotrexate. *J. Biol. Chem.* **257**, 13650–13662.

Bothner-By, A. A., Stephens, R. L., Lee, J., Warren, C. D. & Jeanloz, R. W. (1984). Structure determination of a tetrasaccharide; transient nuclear Overhauser effects in the rotating frame. *J. Am. Chem. Soc.* **106**, 811–813.

Brown, S. C., Weber, P. L. & Mueller, L. (1988). Toward complete ^{1}H-NMR spectra in proteins. *J. Magn. Reson.* **77**, 166–169.

Brünger, A. T. (1992). *X-PLOR 3.1. A System for X-ray Crystallography and NMR,* Yale University Press, New Haven, CT.

Brünger, A. T., Clore, G. M., Gronenborn, A. M. & Karplus, M. (1986). 3-Dimensional structure of proteins determined by molecular dynamics with interproton distance restraints – application to crambin. *Proc. Natl Acad. Sci. USA,* **3**, 3801–3806.

Bystroff, C. & Kraut, J. (1991). Crystal structure of unliganded *Escherichia coli* dihydrofolate reductase ligand induced conformational changes and cooperativity in binding. *Biochemistry,* **30**, 2227–2239.

Bystroff, C., Oatley, S. J. & Kraut, J. (1990). Crystal structures of *Escherichia coli* dihydrofolate reductase. The $NADP^{+}$ holoenzyme and the folate-$NADP^{+}$ ternary complex – substrate binding and a model for the transition-state. *Biochemistry,* **29**, 3263–3277.

Carr, M. D., Birdsall, B., Frenkiel, T. A., Bauer, C. J., Jimenez-Barbero, J., McCormick, J. E., Feeney, J. & Roberts, G. C. K. (1991). Dihydrofolate reductase: sequential resonance assignments using 2D and 3D NMR and secondary structure determination in solution. *Biochemistry,* **30**, 6330–6341.

Champness, J. N., Achari, A., Ballantine, S. P., Bryant, P. K., Delves, C. J. & Stammers, D. K. (1994). Structure of *Pneumocystis carinii* dihydrofolate-reductase to 1.9 Ångstrom resolution. *Structure,* **2**, 915–924.

Cheung, H. T. A., Birdsall, B., Frenkiel, T. A., Chau, D. D. & Feeney, J. (1993). ^{13}C NMR determination of the tautomeric and ionization states of folate in its complexes with *Lactobacillus casei* dihydrofolate reductase. *Biochemistry,* **32**, 6846–6854.

Clore, G. M., Gronenborn, A. M., Nilges, M. & Ryan, C. A. (1987). 3-Dimensional structure of potato carboxypeptidase inhibitor in solution; a study using nuclear magnetic resonance, distance geometry, and restrained molecular dynamics. *Biochemistry,* **26**, 8012–8013.

Clore, G. M., Bax, A., Wingfield, P. T. & Gronenborn, A. M. (1990). Identification and localization of bound internal water in the solution structure of interleukin-1-beta by heteronuclear 3-dimensional ^{1}H rotating-frame Overhauser ^{15}N-^{1}H multiple quantum coherence NMR-spectroscopy. *Biochemistry,* **29**, 5671–5676.

Clore, G. M., Kay, L. E., Bax, A. & Gronenborn, A. M. (1991). 4-Dimensional ^{13}C/^{13}C edited nuclear Overhauser enhancement spectroscopy of a protein in solution; application to interleukin 1-beta. *Biochemistry,* **30**, 12–18.

Cocco, L., Roth, B., Temple, C., Montgomery, J. A., London, R. E. & Blakley, R. L. (1981). Protonated

state of methotrexate, trimethoprim, and pyrimethamine bound to dihydrofolate reductase. *Arch. Biochem. Biophys,* **226**, 567–577.

Dale, G. E., Broger, C., Darcy, A., Hartman, P. G., DeHoogt, R., Jolidon, S., Kompis, I., Labhardt, A. M., Langen, H., Locher, H., Page, M. G. P., Stuber, D., Then, R. L., Wipf, B. & Oefner, C. (1997). A single amino acid substitution in the *Staphylococcus aureas* dihydrofolate reductase determines trimethoprim resistance. *J. Mol. Biol.* **226**, 32–30.

Dann, J. G., Ostler, G., Bjur, R. A., King, R. W., Scudder, P., Turner, P. C., Roberts, G. C. K., Burgen, A. S. V. & Harding, N. G. L. (1976). Large scale purification and characterisation of dihydrofolate reductase from a methotrexate-resistant strain of *Lactobacillus casei*. *Biochem. J.* **157**, 559–571.

Davies, J. F., II, Delcamp, T. J., Prendergast, N. J., Ashford, V. A., Freisheim, J. H. & Kraut, J. (1990). Crystal structures of recombinant human dihydrofolate reductase complexed with folate and 5-deazafolate. *Biochemistry,* **29**, 9467–9479.

Epstein, D. M., Benkovic, S. J. & Wright, P. E. (1995). Dynamics of the dihydrofolate reductase folate complex – catalytic sites and regions known to undergo conformational change exhibit diverse dynamical features. *Biochemistry,* **34**, 11037–11048.

Falzone, C. J., Cavanaugh, J., Cowart, M., Palmer, A. G., III, Matthews, C. R., Benkovic, S. J. & Wright, P. E. (1994). ^{1}H, ^{15}N and ^{13}C resonance assignments, secondary structure, and the conformation of substrate in the binary folate complex of *Eschericia coli* dihydrofolate reductase. *J. Biomol. NMR,* **4**, 349–366.

Feeney, J. (1990). NMR studies of interactions of ligands with dihydrofolate reductase. *Biochem. Pharm.* **40**, 141–152.

Feeney, J. (1996). NMR studies of ligand binding to dihydrofolate reductase and their application in drug design. In *NMR in Drug Design* (Craik, D., ed.), CRC Press, New York.

Feeney, J. & Birdsall, B. (1993). NMR studies of protein-ligand interactions. In *NMR of Biological Macromolecules: A Practical Approach* (Roberts, G. C. K., ed.), Oxford University Press, Oxford.

Fesik, S. W., Gampe, R. T., Jr & Rockway, T. W. (1987). Application of isotope-filtered 2D NOE experiments in the conformational analysis of atrial natriuretic factor (7–23). *J. Magn. Reson.* **74**, 366–371.

Filman, D. J., Bolin, J. T., Matthews, D. A. & Kraut, J. (1982). Crystal structures of *Escherichia coli* and *Lactobacillus casei* dihydrofolate-reductase refined at 1.7 Å resolution. 2. Environment of bound NADPH and implications for catalysis. *J. Biol. Chem.* **257**, 13663–13672.

Freisheim, J. H. & Matthews, D. A. (1984). The comparative biochemistry of dihydrofolate reductase. In *Folate Antagonists as Therapeutic Agents* (Sirotnak, F. M., Burchill, J. J., Ensminger, W. D. & Montgomery, J. A., eds), vol. 1, pp. 69–131, Academic Press, New York.

Frenkiel, T. A., Bauer, C. J., Carr, M. D., Birdsall, B. & Feeney, J. (1990). HMQC-NOESY-HMQC, a 3-dimensional NMR experiment which allows detection of nuclear Overhauser effects between protons with overlapping signals. *J. Magn. Reson.* **90**, 420–425.

Gargaro, A. R., Frenkiel, T. A., Nieto, P. M., Birdsall, B., Polshakov, V. I., Morgan, W. D. & Feeney, J. (1996). NMR detection of arginine-ligand interactions in complexes of *Lactobacillus casei* dihydrofolate reductase. *Eur. J. Biochem.* **238**, 435–439.

Gerothanassis, I. P., Barrie, P. J., Birdsall, B. & Feeney, J. (1996). ^{31}P solid-state NMR measurements used to detect interaction between NADPH and water and to determine the ionization state of NADPH in a protein-ligand complex subjected to low-level hydration. *Eur. J. Biochem.* **235**, 262–266.

Gronenborn, A., Birdsall, B., Hyde, E. I., Roberts, G. C. K., Feeney, J. & Burgen, A. S. V. (1981). Direct observation by NMR of two coexisting conformations of an enzyme-ligand complex in solution. *Nature,* **290**, 273–274.

Hommel, V., Harvey, T. S., Driscoll, P. C. & Campbell, I. D. (1992). Human epidermal growth factor: high resolution solution structure and comparison with human transforming growth factor A. *J. Mol. Biol.* **227**, 271–282.

Hutchinson, E. G. & Thornton, J. M. (1996). PROMOTIF - a program to identify and analyze structural motifs in proteins. *Protein Sci.* **5**, 212–220.

Ikura, M., Bax, A., Clore, G. M. & Gronenborn, A. M. (1990a). Detection of nuclear Overhauser effects between degenerate amide proton resonances by heteronuclear 3-dimensional nuclear-magnetic-resonance spectroscopy. *J. Am. Chem. Soc.* **112**, 9020–9022.

Ikura, M., Kay, L. E., Tschudin, R. & Bax, A. (1990b). 3-Dimensional NOESY-HMQC spectroscopy of a ^{13}C-labeled protein. *J. Magn. Reson.* **86**, 204–209.

Jeener, J., Meier, B. H., Bachmann, P. & Ernst, R. R. (1979). Investigations of exchange processes by two-dimensional NMR. *J. Chem. Phys.* **71**, 4546–4553.

Johnson, J. M., Meiering, E. M., Wright, J. E., Pardo, J., Rosowsky, A. & Wagner, G. (1997). NMR solution structure of the anti tumour compound PT523 and NADPH in the ternary complex with human dihydrofolate reductase. *Biochemistry,* **36**, 4399–4411.

Koradi, R., Billeter, M. & Wüthrich, K. (1996). MolMol – a program for display and analysis of macromolecular structures. *J. Mol. Graphics,* **14**, 51–55.

Krageland, B. B., Andersen, K. V., Madsen, J. C., Knudsen, J. & Poulsen, F. M. (1993). 3-Dimensional structure of the complex between acyl-coenzyme A binding protein and palmitoyl-coenzyme A. *J. Mol. Biol.* **230**, 1260–1277.

Kraulis, P. (1991). MOLSCRIPT – a program to produce both detailed and schematic plots of protein structures. *J. Appl. Crystallog.* **24**, 946–950.

Kumar, A., Wagner, G., Ernst, R. R. & Wüthrich, K. (1981). Buildup rates of the nuclear Overhauser effect measured by 2-dimensional proton magnetic resonance spectroscopy – implications for studies of protein conformation. *J. Am. Chem. Soc.* **103**, 3654–3658.

Kuyper, L. F., Roth, B., Baccanari, D. P., Ferone, R., Beddell, C. R., Champness, J. N., Stammers, D. K., Dann, J. G., Norrington, F. E. A., Baker, D. J. & Goodford, P. J. (1982). Receptor based design of dihydrofolate reductase inhibitors: comparison of crystallographically determined enzyme binding with enzyme affinity in a series of carboxy-substituted trimethoprim analogues. *J. Med. Chem.* **25**, 1120–1122.

Laskowski, R. A., MacArthur, M. W., Moss, D. S. & Thornton, J. M. (1993). PROCHECK: a program to check the stereochemical quality of protein structures. *J. Appl. Crystallog.* **26**, 283–291.

Laskowski, R. A., Rullman, J. A. C., MacArthur, M. W., Kaptein, R. & Thornton, J. M. (1996). AQUA and PROCHECK-NMR: programs for checking the quality of protein structures solved by NMR. *J. Biomol. NMR,* **8**, 477–486.

Lee, H., Reyes, V. M. & Kraut, J. (1996). Crystal structures of *Escherichia coli* dihydrofolate reductase complexed with 5-formyltetrahydrofolate (folinic acid) in 2 space groups. Evidence for enolization of pteridine O4. *Biochemistry,* **35**, 7012–7020.

Lewis, W. S., Cody, V., Galitsky, N., Luft, J. R., Pangborn, W., Chunduros, S. K., Spencer, H. T., Appleman, J. R. & Blakley, R. L. (1995). Methotrexate resistant variants of human dihydrofolate reductase with substitutions of leucine-22; kinetics, crystallography, and potential as selectable markers. *J. Biol. Chem.* **270**, 5057–5064.

Live, D. H., Davis, D. G., Agosta, W. C. & Cowburn, D. (1984). Observation of 1000-fold enhancement of ^{15}N NMR via proton detected multiquantum coherences: studies of large peptides. *J. Am. Chem. Soc.* **106**, 1939–1941.

Marion, D., Driscoll, P. C., Kay, L. E., Wingfield, P. T., Bax, A., Gronenborn, A. M. & Clore, G. M. (1989a). Overcoming the overlap problem in the assignment of ^{1}H NMR spectra of larger proteins by use of 3-dimensional heteronuclear ^{1}H-^{15}N Hartmann-Hahn multiple quantum coherence and nuclear Overhauser multiple quantum coherence spectroscopy – application to interleukin-1-beta. *Biochemistry,* **28**, 6150–6156.

Marion, D., Kay, L. E., Sparks, S. W., Torchia, D. A. & Bax, A. (1989b). Three-dimensional heteronuclear NMR of ^{15}N-labelled proteins. *J. Am. Chem. Soc.* **111**, 1515–1517.

Martorell, G., Gradwell, M. J., Birdsall, B., Bauer, C. J., Frenkiel, T. A., Cheung, H. T. A., Polshakov, V. I., Kuyper, L. & Feeney, J. (1994). Solution structure of bound trimethoprim in its complex with *Lactobacillus casei* dihydrofolate reductase. *Biochemistry,* **33**, 12416–12426.

Matthews, D. A., Bolin, J. T., Burridge, J. M., Filman, D. J., Volz, K. W., Kaufman, B. T., Beddell, C. R., Champness, J. N., Stammers, D. K. & Kraut, J. (1985a). Refined crystal structures of *Escherichia coli* and chicken liver dihydrofolate reductase containing bound trimethoprim. *J. Biol. Chem.* **260**, 381–391.

Matthews, D. A., Bolin, J. T., Burridge, J. M., Filman, D. J., Volz, K. W. & Kraut, J. (1985b). Dihydrofolate reductase – the stereochemistry of inhibitor selectivity. *J. Biol. Chem.* **260**, 392–399.

McDonald, I. K. & Thornton, J. M. (1994). Satisfying hydrogen bonding potential in proteins. *J. Biol. Chem.* **238**, 777–793.

McTigue, M. A., Davies, J. F., II, Kaufmann, B. T. & Kraut, J. (1993). Crystal structures of chicken liver dihydrofolate reductase – binary thioNADP^{+} and ternary thioNADP^{+} biopterin complexes. *Biochemistry,* **32**, 6855–6862.

Morgan, W. D., Birdsall, B., Polshakov, V. I., Sali, D., Kompis, I. & Feeney, J. (1995). Solution structure of a brodimoprim analogue in its complex with *Lactobacillus casei* dihydrofolate reductase. *Biochemistry,* **34**, 11690–11702.

Nieto, P. M., Birdsall, B., Morgan, W. D., Frenkiel, T. A., Gargaro, A. R. & Feeney, J. (1997). Correlated bond rotations in interactions of arginine residues with ligand carboxylate groups in protein ligand complexes. *FEBS Letters,* **405**, 16–20.

Nilges, M. (1995). Calculation of protein structures with ambiguous distance restraints. Automated assignment of ambiguous NOE crosspeaks and disulphide connectivities. *J. Mol. Biol.* **245**, 645–660.

Nilges, M., Gronenborn, A. M., Brünger, A. T. & Clore, G. M. (1988). The determination of three-dimensional structures by simulated annealing with interproton distance restraints – application to crambin, potato carboxypeptidase inhibitor and barley serine inhibitor-2. *Protein Eng.* **2**, 27–38.

Nilges, M., Kuszewski, J. & Brünger, A. T. (1991). Sampling properties of simulated annealing and distance geometry. In *Computational Aspects of the Study of Biological Macromolecules by NMR* (Hoch, J. C., ed.), Plenum Press, New York.

Oefner, C., D'arcy, A. & Winkler, F. K. (1988). Crystal structure of human dihydrofolate reductase complexed with folate. *Eur. J. Biochem.* **174**, 377–385.

Otting, G. & Wüthrich, K. (1990). Heteronuclear filters in 2-dimensional [^{1}H, ^{1}H] NMR-spectroscopy – combined use with isotope labeling for studies of macromolecular conformation and intermolecular interactions. *Quart. Rev. Biophys.* **23**, 39–96.

Otting, G., Senn, H., Wagner, G. & Wüthrich, K. (1986). Editing of 2D ^{1}H NMR spectra using X half-filters – combined use with residue-selective ^{15}N labeling of proteins. *J. Magn. Reson.* **70**, 500–505.

Polshakov, V. I., Birdsall, B., Gradwell, M. J. & Feeney, J. (1995a). The use of PM3 SCF MO quantum mechanical calculations to refine NMR-determined structures of complexes of antifolate drugs with dihydrofolate reductase in solution. *J. Mol. Struct.* **357**, 207–216.

Polshakov, V. I., Frenkiel, T. A., Birdsall, B., Soteriou, A. & Feeney, J. (1995b). Determination of stereospecific assignments, torsion-angle constraints, and rotamer populations in proteins using the program AngleSearch. *J. Magn. Reson. ser. B,* **108**, 31–43.

Presta, L. G. & Rose, G. D. (1988). Helix signals in proteins. *Science,* **240**, 1632–1641.

Reyes, V. M., Sawaya, M. R., Brown, K. A. & Kraut, J. (1995). Isomorphous crystal structures of *Escherichia coli* dihydrofolate reductase complexed with folate, 5-deazafolate, and 5,10 dideazatetrahydrofolate; mechanistic implications. *Biochemistry,* **34**, 2710–2723.

Roth, B. & Cheng, C. C. (1982). Recent progress in the medicinal chemistry of 2,4-diaminopyrimidines. *Prog. Med. Chem.* **19**, 1–58.

Rychaert, J.-P., Ciccotti, G. & Berendsen, H. J. C. (1977). Numerical-integration of cartesian equations of motion of a system with constraints: molecular dynamics of N-alkanes. *J. Comput. Phys.* **23**, 327–341.

Sawaya, M. R. & Kraut, J. (1997). Loop and subdomain movements in the mechanism of *E. coli* dihydrofolate reductase: crystallographic evidence. *Biochemistry,* **36**, 586–603.

Searle, M. S., Forster, M. J., Birdsall, B., Roberts, G. C. K., Feeney, J., Cheung, H. T. A., Kompis, I. & Geddes, A. J. (1988). Dynamics of trimethoprim bound to dihydrofolate reductase. *Proc. Natl Acad. Sci. USA,* **85**, 3787–3791.

Shaka, A. J., Barker, P. B. & Freeman, R. (1985). Computer-optimized decoupling scheme for wideband applications and low-level operation. *J. Magn. Reson.* **64**, 547–552.

Sklenar, V., Piotto, M., Leppik, R. & Saudek, V. (1993). Gradient-tailored water suppression for ^{1}H-^{15}N HSQC experiments optimised to retain full sensitivity. *J. Magn. Reson. ser. A,* **102**, 241–245.

Soteriou, A., Carr, M. D., Frenkiel, T. A., McCormick, J. E., Bauer, C. J., Sali, D., Birdsall, B. & Feeney, J. (1993). 3D $^{13}C/^{1}H$ NMR-based assignments for side chain resonances of *Lactobacillus casei* dihydrofolate reductase. Evidence for similarities between the solution and crystal structures of the enzyme. *J. Biomol. NMR,* **3**, 535–546.

States, D. J., Haberkorn, R. A. & Ruben, D. J. (1982). A two-dimensional nuclear Overhauser experiment with pure absorption phase in four quadrants. *J. Magn. Reson.* **48**, 286–292.

Stockman, B. J., Nirmala, N. R., Wagner, G., Delcamp, T. J., De Yarmen, M. T. & Freisheim, J. H. (1992). Sequence-specific ^{1}H and ^{15}N resonance assignments for human dihydrofolate reductase in solution. *Biochemistry,* **31**, 218–229.

Sutcliffe, M. J. (1993). Representing an ensemble of NMR derived protein structures by a single structure. *Protein Sci.* **2**, 936–944.

Sutton, P. A., Cody, V. & Smith, G. D. (1986). Crystal structure of methotrexate tetrahydrate. *J. Am. Chem. Soc.* **108**, 4155–4158.

Vuister, G. W. & Bax, A. (1993). Quantitative J correlation – a new approach for measuring homonuclear 3-bond J(HN-Hα) coupling-constraints in ^{15}N enriched proteins. *J. Am. Chem. Soc.* **115**, 7772–7777.

Wagner, G., Braun, W., Havel, T. F., Schaumann, T., Go, N. & Wüthrich, K. (1987). Protein structures in solution by nuclear magnetic-resonance and distance geometry – the polypeptide fold of the basic pancreatic trypsin-inhibitor determined using two different algorithms, DISGEO and DISMAN. *J. Mol. Biol.* **196**, 611–639.

Wang, A. C. & Bax, A. (1995). Reparameterization of the Karplus relation for $^{3}J(H^{\alpha}\text{-}N)$ and $^{3}J(H^{N}\text{-}C')$ in peptides from uniformly enriched human ubiquitin. *J. Am. Chem. Soc.* **117**, 1810–1813.

Warren, M. S., Brown, K. A., Farnum, M. F., Howell, E. E. & Kraut, J. (1991). Investigation of the functional role of tryptophan-22 in *Escherichia coli* dihydrofolate reductase by site-directed mutagenesis. *Biochemistry,* **30**, 11092–11103.

Wishart, D. S., Bigam, C. G., Yao, J., Abildgaard, F., Dyson, H. J., Oldfield, E., Markley, J. L. & Sykes, B. D. (1996). ^{1}H, ^{13}C and ^{15}N chemical shift referencing in biomolecular NMR. *J. Biomol. NMR,* **6**, 135–140.

Zuiderweg, E. R. P., McIntosh, L. P., Dahlquist, F. W. & Fesik, S. W. (1990). 3-Dimensional ^{13}C resolved proton NOE spectroscopy of uniformly ^{13}C-labeled proteins for the NMR assignment and structure determination of larger molecules. *J. Magn. Reson.* **86**, 210–216.

Zuiderweg, E. R. P., Petros, A. M., Fesik, S. W. & Oleniczak, E. T. (1991). 4-Dimensional [^{13}C, ^{1}H, ^{13}C, ^{1}H] HMQC-NOE-HMQC NMR-spectroscopy-resolving tertiary NOE restraints in the spectra of larger proteins. *J. Am. Chem. Soc.* **113**, 370–371.

Edited by P. E Wright

(Received 11 July 1997; received in revised form 2 December 1997; accepted 3 December 1997)

http://www.hbuk.co.uk/jmb

Supplementary material for this paper comprising one Table is available from JMB Online.